Quantitative comparison of methods used to estimate methane emissions from small point sources

Stuart N. Riddick[1], Riley Ancona[1], Clay Bell[1], Aidan Duggan[1], Tim Vaughn[1], Kristine Bennett[1] and Dan Zimmerle[1]

[1] The Energy Institute, Colorado State University, Fort Collins, CO, 80524, USA

Correspondence to: Stuart.Riddick@colostate.edu

Abstract Recent interest in quantifying trace gas emissions from point sources, such as measuring methane (CH_4) emissions from oil and gas wells, has resulted in several methods being used to estimate emissions from sources with emission rates below 200g CH_4 hour^{-1}. The choice of measurement approach depends on how close observers can get to the source, the instruments available and the meteorological/micrometeorological conditions. As such, static chambers, dynamic chambers, Hi Flow measurements, Gaussian plume (GP) modelling and backward Lagrangian stochastic (bLs) models have all been used, but there is no clear understanding of the accuracy or precision of each method. To address this, we copy the experimental design for each of the measurement methods to make single field measurements of a known source, to simulate single measurement field protocol, and then make repeat measurements to generate an understanding of the accuracy and precision of each method. Here, ~~for comparison,~~ we present estimates for the average percentage difference between the measured emission and the known emission~~, *A*, and the average percentage difference~~ for three repeat measurements, A_r, for emissions of 40 to 200 g CH_4 h^{-1}. The static chamber data were not presented because of safety concerns during the experiments. Both the dynamic chamber (A_r = -10%, -8%, -10% at emission rates of 40, 100 and 200 g CH_4 h^{-1}, respectively) and Hi Flow (A_r = -18%, -16%, -18%) repeatedly underestimate the emission, but the dynamic chamber had better accuracy. The standard deviation of emissions from these direct measurement methods remained relatively constant for emissions between 40 and 200 g CH_4 h^{-1}. For the far field methods, the bLs method generally underestimated emissions (A_r = +6%, -6%, -7%) while the GP method significantly overestimated the emissions (A_r = +86%, +57%, +29%) despite using the same meteorological and concentration data as input. Variability in wind speed, wind direction and atmospheric stability over the 20-minute averaging period are likely to propagate through to large variability in the emission estimate, making these methods less precise than the direct measurement methods. ~~Our results show that, even though the dynamic chamber repeatedly underestimates the emission, it is the most accurate for a single measurement and the accuracy improves with subsequent measurements (*A* = -11%, A_r = -10%). The single HiFlow emission estimate was also an underestimate, however, poor instrument precision resulted in reduced accuracy of emission estimate to becomes less accurate after repeat measurements (*A* = -16%, A_r = -18%). Of the far field methods, the bLs method underestimated emissions both for single and repeat measurements (*A* = -11%, A_r = -7%) while the GP method significantly overestimated the emissions (*A* = 33%, A_r = 29%) despite using the same meteorological and concentration data as input. Additionally, our results show that the accuracy and precision of the emission estimate increases as the flow rate of the source is increased for all methods.~~ To our knowledge this is the first time that methods for measuring CH_4 emissions from point sources ~~less than~~between 40 and 200 g CH_4 h^{-1} have been quantitively assessed against a known reference source and each other.

1 Introduction

Methane (CH_4) gas is a powerful greenhouse gas with a greenhouse warning potential 84 times larger than carbon dioxide over 100 years. Quantification of CH_4 emissions from abandoned wells has recently become an area of interest as studies suggest over 200 Gg CH_4 yr^{-1} is emitted from 2.2 million abandoned wells in the US alone (US EPA, 2021). Quantifying and then plugging these wells makes them an attractive target for achieving goals set out in the Paris Agreement (Nisbet et al., 2020). Additionally, private companies are beginning initiatives to generate revenue through carbon credits gained by plugging wells and accurate quantification is essential for realizing the capital.

As there are millions of abandoned wells globally, there is a growing need to measure as many wells as quickly as possible to identify the most emissive wells. Typically, an emission from an abandoned well can be considered as an above-ground point source that is relatively small in emission size, up to 180 g CH_4 $hour^{-1}$ (Riddick et al., 2019a; Pekney et al., 2018; Townsend-Small et al., 2016; Boothroyd et al., 2016). Other emission sources, such as emissions pipeline leakage, are fundamentally different in behavior, where gas travels through the soil and forms an area emission at the surface, these sources require different methods for estimating the emission, e.g. mass balance or eddy covariance. Area emissions could form if a plugged well leaks from corrosion of the borehole casing, but this will not be discussed in this study.

Several methods are being used to measure emissions from these smaller point sources, i.e. less than 180 g CH_4 $hour^{-1}$. The chosen measurement approach depends on how close an observer can get to the source, instrumentation availability and the meteorological/micrometeorological conditions at the measurement site. Measurement methods can be classed as direct, i.e. touching/enclosing the source, and downwind measurements where access is not possible. Direct methods include static chambers (Livingston and Hutchinson, 1995), dynamic flux chambers (Riddick et al., 2019a, 2020b; Aneja et al., 2006) and Hi Flow sampling (Pekney et al., 2018; Allen et al., 2013; Brantley et al., 2015). While downwind methods include Gaussian-based plume models (Baillie et al., 2019; Caulton et al., 2014; Riddick et al., 2019b, 2020a; Edie et al., 2020; Bell et al., 2017) and Lagrangian dispersion models (Riddick et al., 2019b, 2017; Denmead, 2008; Flesch et al., 1995). Emissions calculated using the majority of these methods have not been comprehensively compared using to controlled emission source rates.

Other quantification methods are generally unsuitable for measuring emissions from abandoned wells. Infra-red cameras, such as FLIR cameras, cannot be used to quantify emission and have difficultly detecting plume smaller emissions (Zimmerle et al., 2020). Mass balance approaches are unlikely to detect the small and narrow plume from the abandoned well. Tracer release is technically demanding, takes a long time to make a single measurement and requires road access for measurement. Remote sensing has typical detection limits of 10+ kg CH_4 h^{-1} for aircraft (Duren et al., 2019), 100+ kg CH_4 h^{-1} for satellites (Cooper et al., 2022) and unsuitable for these types of emission source. As such, these other quantification methods will not be investigated in this study.

~~Recent interest in quantifying trace gas emissions from point sources, such as measuring methane (CH_4) emissions from oil and gas wells (Omara et al., 2016; Pekney et al., 2018; Riddick et al., 2019a; Vaughn et al., 2018; Alvarez et al., 2018; Zavala-Araiza et al., 2021), has resulted in several methods being used to measure emissions from smaller point sources, i.e. less than 200g CH_4 $hour^{-1}$. Measurement approaches depend on how close observers can get to the source, due to access restrictions, instrumentation availability and the meteorological/micrometeorological conditions at the measurement site. Broadly put, these methods can be classed as direct measurements, i.e. touching/enclosing the source, and downwind measurements where access is not possible. Direct methods include: static chambers (Livingston and Hutchinson, 1995; Kang et al., 2014), dynamic flux chambers (Riddick et al., 2019a, 2020; Aneja et al., 2006) and Hi-Flow sampling (Pekney et al., 2018; Allen et al., 2013; Brantley et al., 2015). While downwind methods include: Gaussian plume models (Baillie et al., 2019; Caulton et al., 2014; Riddick et al., 2017; Edie et al., 2020; Bell et al., 2017) and Lagrangian dispersion models (Riddick et al., 2019a, 2017; Denmead, 2008; Flesch et al., 1995).~~

~~Despite the interest in developing methods, emissions calculated using these methods have not been comprehensively compared using a known emission source, even though the results of these studies are being used to guide policy.~~

~~Static chambers have been used to estimate CH_4 emissions from abandoned wells that are very small sources (0.6 mg hr^{-1}) to those that are much larger (90 g hr^{-1}) (Kang et al., 2014). This method is relatively simple, where a container of a known volume (V, m^3) is place over the emission source and the change in concentration (C, g m^{-3}) inside the container over time (t, s) can be used to calculate the emission (Q, g s^{-1}; Equation 1). Kang et al. (2014) reported using a gas chromatograph after the measurement campaign to assay CH_4 concentrations taken from the chamber at time intervals. Therefore, the static chamber method requires no power, apart from batteries to run a fan in the chamber and is very portable. Major shortcomings of this method are the uncertainty caused by incomplete mixing of methane in the chamber, estimated at a factor of 2 (Kang et al., 2014), and large emission sources can result in the concentration inside the chamber exceeding the CH_4 lower explosive limit (LEL).~~

$$\cancel{Q = \frac{dC}{dt} . V \qquad \text{(Equation 1)}}$$

~~To address LEL issues inside the chamber, a dynamic flux method has also been used to measure CH_4 leakage from abandoned and active oil and gas wells (Riddick et al., 2019a). Like the static chamber, the dynamic chamber comprises of a container enclosing the source and a propeller is used to circulate the air. Additionally, a flow of air is passed through the chamber, which reduces the likelihood of exceeding LEL inside the chamber. Unlike the static chamber, the CH_4 concentration becomes stable after a period of time depending on the source emission rate. The CH_4 flux (Q, g s^{-1}) is calculated (Equation 2) from the CH_4 concentration at steady state (C_{eq}, g m^{-3}), the background CH_4 concentration (C_b, g m^{-3}) in the air used to flush the chamber, the height of the chamber (h, m), the flow of air through the chamber (q, m^3 s^{-1}), the area of the chamber (a, m^2) and the volume of the chamber (V, m^3) (Aneja et al., 2006; Riddick et al., 2019a). As well as improving the safety, the dynamic chamber reduces the theoretical uncertainty in emission rate to ± 7% (Riddick et al., 2019a), however, the added power requirement of a pump means the dynamic chamber is less portable than the static chamber. Methane emissions have been calculated using this method between 4 µg CH_4 hr^{-1} and 100 g CH_4 hr^{-1} (Riddick et al., 2019a).~~

$$\cancel{Q = \frac{(C_{eq} - C_b) \cdot h \cdot q \cdot a}{V} \qquad \text{(Equation 2)}}$$

~~Another way of addressing the issue of enclosing methane at concentrations approaching LEL is to use a Hi-Flow sampler. As the name suggests, a Hi-Flow sampler draws high volumes of air – typical rates are 300 $l\ min^{-1}$ – into a measurement chamber, where the concentration of CH_4 in the air is measured and then calculates an emission rate. The current commercial HiFlow sampler uses two sensors, a catalytic oxidation sensor to measure CH_4 concentrations between 0 and 5% and a thermal conductivity sensor between 5% and 100% CH_4. These concentration measurements are then used to calculate emissions between 1 and 140 g CH_4 hr^{-1} (Equation 3), at an accuracy of ± 10%. A recent independent study found the Bacharach HiFlow Sampler to be a suitable instrument for measuring CH_4 emissions if operated correctly within its limitations, but found the uncertainty largest when measuring at the transition of the sensors, i.e. ~5% methane (Connolly et al., 2019).~~

$$\cancel{Q = F . (X_s - X_b) \qquad \text{(Equation 3)}}$$

~~In some circumstances, access and safety restrictions mean that direct measurements are impossible, and an observer must use a far-field method to measure the emissions remotely. The most widely used of these far-field approaches is the Gaussian plume (GP) model. First used in the 1940s, a GP model describes the concentration of a gas as a function of distance downwind from a point source (Seinfeld and Pandis, 2016). When a gas is emitted from the source, it is entrained in the prevailing ambient air flow and disperses laterally and vertically with time, forming a dispersed concentration cone. The concentration of the gas (X, µg m^{-3}), at any point x meters downwind of the source, y meters laterally from the center line of the plume and z meters above ground level can be calculated (Equation 4) using the emission rate (Q, g s^{-1}), the height of the source (h_s, m) and the Pasquill-Gifford stability~~

~~class (PGSC) as a measure of air stability. The standard deviation of the lateral (σ_y, m) and vertical (σ_z, m) mixing ratio distributions are calculated from the PGSC of the air (Pasquill, 1962; Busse and Zimmerman, 1973; US EPA, 1995). The GP model assumes that the vertical eddy diffusivity and wind speed are constant and there is total reflection of CH_4 at the surface. The GP is the simplest of the far-field methods and assumes that the emissions are well-defined plumes injected above the near-surface turbulent layer from point sources and not affected by aerodynamic obstructions that cause mechanical turbulence at the surface. However, in most situations there are aerodynamic obstacles and plumes are rarely perfectly Gaussian in shape. Another shortcoming of the GP model is the parameterization of the PGSC, which are discrete values and incorrectly assigning them can lead to significant uncertainty. Generally, speaking the GP is rarely used for emissions less than 100 g CH4 h^{-1}. However, an example of using a GP model is its use estimating CH_4 emissions from oil production platforms in the North Sea, where emissions ranged from 10 to 80 kg CH_4 hr^{-1} with an uncertainty of ± 45% (Riddick et al., 2019b)~~

$$X(x,y,z) = \frac{Q}{2\pi u \sigma_y \sigma_z} e^{-\frac{y^2}{(2\sigma_y)^2}} \left(e^{-\frac{(z-h_s)^2}{(2\sigma_z)^2}} + e^{-\frac{(z+h_s)^2}{(2\sigma_z)^2}} \right) \quad \text{(Equation 4)}$$

~~As an alternative to the GP model, Lagrangian dispersion models can be used to calculate the emission of a source. In a backward Lagrangian stochastic (bLS) model, the measurement position, gas concentration, meteorology and micrometeorology are known inputs and the model works iteratively backwards to simulate the motion of the air parcel, this is then used to infer the rate of emission from the source (Flesch et al., 1995). For given meteorological conditions, the model calculates the ratio of downwind concentration to emission, $(C/Q)_{sim}$, depending on the size and location of the source. The emission rate (Q, g m^{-2} s^{-1}) is then inferred from the measured gas concentration (X_m, g m^{-3}) and the background gas concentration (X_b, g m^{-3}) (Equation 5). The bLS models can be used to calculate the emissions from point or area sources in a range of micrometeorological conditions. However, a major shortcoming of the model is its inability to adequately model emissions from sources with complex topography or near large objects, such as buildings. This can be mitigated by measuring far away from the source over a relatively flat fetch, but an accurate measurement of the micrometeorology is required. As an example, CH_4 emissions from individual point sources on oil and gas infrastructure have been estimated using a bLS model between 4 µg CH_4 hr^{-1} and 3 kg CH_4 hr^{-1} with an uncertainty of ± 38% (Riddick et al., 2019a)~~

$$Q = \frac{X_m - X_b}{\left(\frac{C}{Q}\right)_{sim}} \quad \text{(Equation 5)}$$

In general, as access becomes more restricted, emission rates larger, or safety concerns increase (such as the co-emission of harmful gases), the method~~s~~ used to estimate the CH_4 emission rate of a source ~~become more complex~~must be carefully considered. From experience and the response of a 4-gas monitor, working close enough to measure emissions greater than 200 g CH_4 h^{-1} for many of these methods (especially the chambers and Hi Flow) can be unsafe, therefore this study is limited to quantifying CH_4 emissions between the lowest flow METEC can produce (40 g CH_4 h^{-1}) and the highest flow we feel comfortable measuring with these methods (200 g CH_4 h^{-1}). Putting these emission ranges into real-word context, the maximum emission from unplugged and abandoned wells was measured at 177 g CH_4 h^{-1} in West Virginia (Riddick et al., 2019a), 175 g CH_4 h^{-1} in Pennsylvania (Pekney et al., 2018), 146 g CH_4 h^{-1} across the US (Townsend-Small et al., 2016) and 35 g CH_4 h^{-1} in the UK (Boothroyd et al., 2016). As most of the methods presented here require access to the source, we considered 200 g CH_4 h^{-1} to be a sensible limit to the emission rate and is larger than the emissions observed by many previous studies. ~~We~~ Therefore, ~~limit~~ the scope of this study is limited to estimating CH_4 emissions from a single point source that we would realistically be able to approach and measure, i.e. ~~less than~~between 40 and 200 g CH_4 h^{-1}.

The study compares each method's accuracy against known emission rates. Explicitly, our objectives are: 1) ~~Copy~~ Reproduce the experimental design for each of the measurement methods; 2) Conduct single measurements as a researcher would do in the field

by taking measurements to generate a single emission estimate from a point source and compare this to known emission rate; 3) Conduct repeat measurements to generate an understanding of the accuracy and precision of the methods that can help inform on the cost-benefit implications of repeat experiments; and 4) Make recommendations on the suitability of each method for measuring emissions from relatively small point sources. We add the caveat that we will only present data from measurement methodologies can be conducted safely, wearing PPE as regulated at the Colorado State University Methane Emissions Technology Evaluation Center (METEC) facility in Fort Collins, CO, USA (steel toe boot, FR overalls, hard hat, safety glasses and 4-gas monitor). To our knowledge this is the first time that methods for measuring CH_4 emissions from point sources ~~less than~~between 40 and 200 g CH_4 h^{-1} have been quantitively assessed against a known reference source and each other.

2 Methods

Each of the methods, static chambers, dynamic chambers, Hi-Flow, bLs and GP, are tested at ~~the Colorado State University Methane Emissions Technology Evaluation Center (~~METEC~~) site~~ in Fort Collins, CO, USA. METEC can reproduce the range of CH_4 emissions typically seen from individual point sources at oil and gas operations, i.e. between 20 g CH_4 hr^{-1} and 40 kg CH_4 hr^{-1}, from realistic locations on O&G equipment. At the METEC site, compressed natural gas, with methane compositions ranging from 85 to 95%vol, is supplied from two 145 L cylinders and flow rates controlled using a pressure regulator and precision orifices. For the purposes of this study, where we are comparing the ability of each method to estimate the emission from a point source, we will constrain the known emission rates to those that can be measured safely, i.e. ~~up to~~between 40 and 200 g CH_4 hr^{-1}. To accomplish this, CH_4 emission rates will be set from a point source (diameter 6 mm) at 20 cm above the ground at 40, 100 and 200 g CH_4 hr^{-1}.

Two instruments are used to report CH_4 mixing ratios: the Picarro (ww.picarro.com) GasScouter G4301 mobile gas concentration analyser and the Agilent (www.aglient.com) 7890B Flame-Ionization Detector Gas Chromatograph (GC-FID). The Picarro GasScouter reports CO_2, H_2O and CH_4 mixing ratios every 3 s, with a precision (300s, 1σ) for CH_4 of 300 ppb over an operating range of 0 to 800 ppm. The Agilent 7890B gas chromatograph-flame ionization detector (GC-FID), as used here, has a detection limit of 1.5 ppb and linear dynamic range from 1 ppm to 100% CH_4. The instrument was calibrated every 10 samples using a 5,000 ppm gas standard (accuracy of standard ± 5%). The GC-FID was checked for linearity before and after each set of measurements using zero-air, 5,000 ppm, 2.5% and 100% CH_4.

2.1 Static Chamber

The static chambers method is relatively simple, where a container of a known volume (V, m^3) is placed over the emission source and the change in concentration (C, g m^{-3}) inside the container over time (t, s) can be used to calculate the emission (Q, g s^{-1}; Equation 1). The static chamber method requires no power, apart from batteries to run a fan in the chamber and is very portable. The major shortcoming of this method is that large emission sources can result in the concentration inside the chamber exceeding the CH_4 lower explosive limit (LEL).

$$Q = \frac{dC}{dt} . V \qquad \text{(Equation 1)}$$

Following method descriptions presented in Pihalatie et al. (2013) and Collier et al. (2014), the static chamber is made by enclosing air within a fixed volume over the emission source (Figure 1A). A fan was~~is~~ secured inside the chamber and used to circulate the air following the method of (Riddick et al. 2019a) to ensure the air inside the chamber was fully mixed. As the experiment was conducted at METEC, 120 V mains power was used, however, in a remote locations power can be supplied by anything capable

of delivering a stable 12 V output (e.g. battery). When the chamber is sealed with the ground, following Riddick et al. (2019a), an air sample is drawn using a gas syringe. D~~. ~~uring ~~During~~ the experiment at least three further air samples are taken at regular intervals (Pihlatie et al., 2013; Collier et al., 2014), the time interval was pre-calculated depending on the emission rate to ensure the increase in concentration was linear. The emission is then calculated from the linear increase in concentration over time. ~~Three~~ Two sizes of static chambers were used in this experiment (~~:~~ 0.12 m^3 and~~,~~ 0.5 m^3 ~~and 1.2 m^3~~; Figure 1), the chambers were made from rigid plastic cylindrical chambers, with heights approximately 1.5 times the chamber's diameter. ~~.~~ The chambers sizes was based on a measurable concentration change over time for given release rates, however, it is unlikely that the larger size is practical for field deployment.~~The largest chamber reportedly used by Kang et al. (2014) was 2 m^3, however, we found it was impossible to maintain a ground seal with a chamber of this size in anything other than zero wind (0 m s^{-1}) wind conditions.~~ During any wind the chamber acted as a sail and the larger chamber lifted from the ground, therefore, smaller chambers are better in the wind but quickly fill with gas making measurement difficult. In each case, the chamber was placed over a point source 20 cm above the ground emitting gas at approximately 40, 100 and 200 g CH_4 hr^{-1}. During the experiment, four samples of 25 ml of air were drawn from the chamber using a 50 ml gas syringe at equal time intervals (Pihlatie et al., 2013; Collier et al., 2014). The air samples were injected into glass vials containing 30 ml of nitrogen and then stored in a fridge before the CH_4 concentrations were measured using the GC-FID. All samples were measured within two ~~weeks~~ hours of collection. All experiments were repeated three times.

The minimum time between air sampling was set at one minute to ensure that the correct vial could be found and the sample outlet purged of gas. When sampling times were less, the experiment became too rushed and errors occurred. Additionally, as a health and safety precaution, a handheld CH_4 sensor, HXG-2D (Sensit Technologies, USA, www.gasleaksensors.com; detection limit 10 ppm and range 0 to 40,000 ppm)~~)~~, was placed in the chamber and if the CH_4 concentration exceeded the lower explosive limit before three samples were taken the test was abandoned.

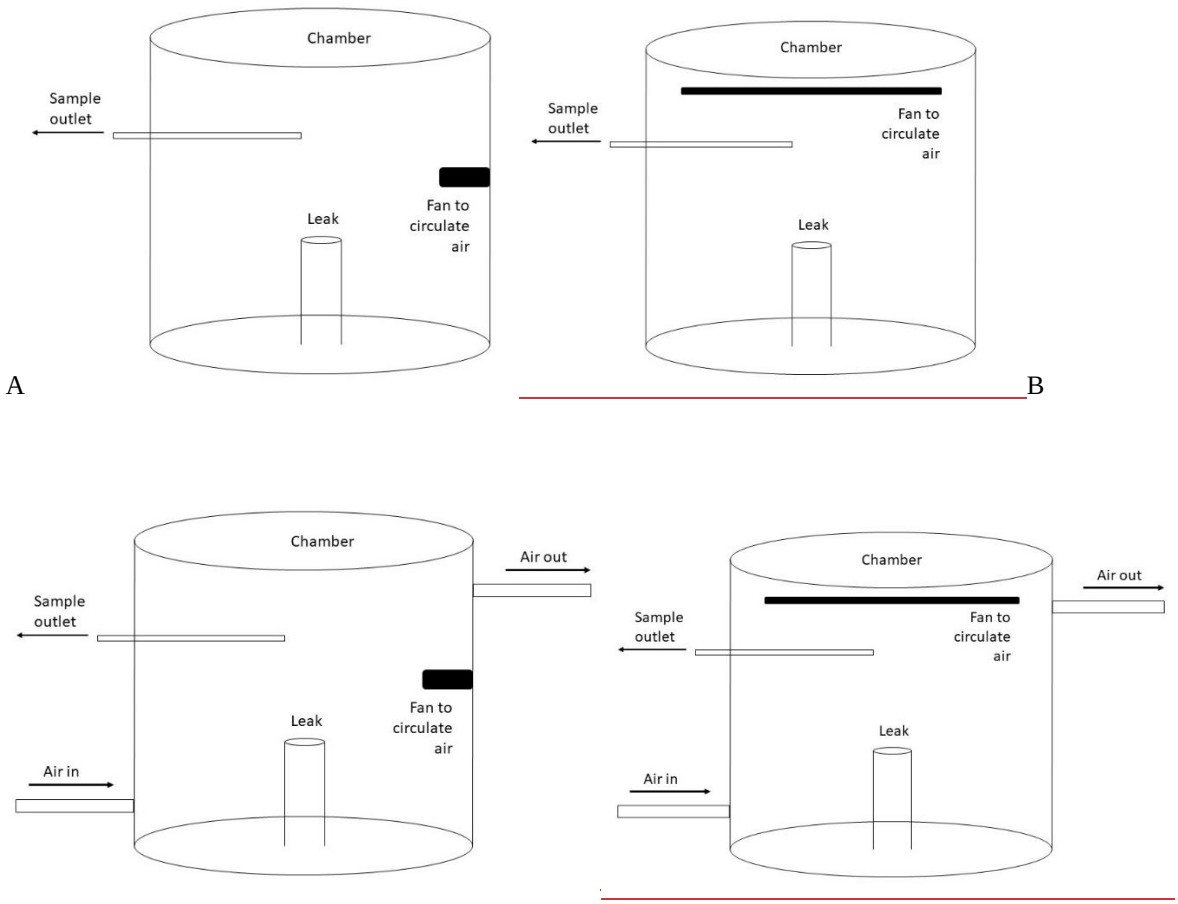

Figure 1 Schematics of the A. Static chamber and B. Dynamic flux chamber.

2.2 Dynamic Chamber

To address LEL issues inside the chamber, a dynamic flux method has also been used to measure CH_4 leakage from abandoned and active oil and gas wells (Riddick et al., 2019a). Like the static chamber, the dynamic chamber comprises of a container enclosing the source and a propeller is used to circulate the air. Additionally, a flow of air is passed through the chamber, which reduces the likelihood of exceeding LEL inside the chamber. Unlike the static chamber, the CH_4 concentration becomes stable after a period of time depending on the source emission rate. When the chamber reached steady state, three air samples were taken from inside the chamber. A background air sample was taken outside the chamber as the chamber approached steady state. The methane concentration in all air samples was measured using a gas chromatography. The CH_4 flux (Q, g s^{-1}) is calculated (Equation 2) from the CH_4 concentration at steady state (C_{eq}, g m^{-3}), the background CH_4 concentration (C_b, g m^{-3}) in the air used to flush the chamber, the height of the chamber (h, m), the flow of air through the chamber (q, m^3 s^{-1}), the area of the chamber (a, m^2) and the volume of the chamber (V, m^3) (Aneja et al., 2006; Riddick et al., 2019a). As well as improving the safety, the dynamic chamber reduces the theoretical uncertainty in emission rate to ± 7% (Riddick et al., 2019a), however, the added power requirement of a pump means the dynamic chamber is less portable than the static chamber. Methane emissions have been calculated using this method between 4 µg CH_4 hr^{-1} and 100 g CH_4 hr^{-1} (Riddick et al., 2019a).

$$Q = \frac{(C_{eq} - C_b) \cdot h \cdot q \cdot a}{V} \qquad \text{(Equation 2)}$$

A single chamber 0.12 m^3 was used for testing the dynamic chamber method. The plastic chamber, open at one end, was placed over known leaks of approximately 40, 100 and 200 g CH_4 hr^{-1} and air was passed through the chamber at a constant rate of 67 l min^{-1}, following the method of Riddick et al. (2019). As the experiment was conducted at METEC, 120 V mains power was used, however, in a remote location power can be supplied by anything capable of delivering a stable 12 V output. The chamber was left until the CH_4 concentration inside had become constant, as measured by the HXG-2D sensor. When steady state was reached, three sample of 25 ml of air were drawn from the chamber using a 50 ml gas syringe injected into glass vials containing 30 ml of nitrogen. As with the samples from the static chamber, the vials were measured within two hours of collection. All experiments were repeated three times.~~stored in a fridge and measured withing two weeks of collection.~~ Following the methods of Aneja et al. (2006) and Riddick et al. (2019; 2020), the emission is calculated from the steady state gas concentration using Equation 2.

2.3 Hi-Flow

Another way of addressing the issue of enclosing methane at concentrations approaching LEL is to use a Hi Flow sampler. A Hi Flow sampler draws high volumes of air into a measurement chamber, where the concentration of CH_4 in the air is measured and the emission rate calculated (Equation 3). The Bacharach Hi Flow Sampler (Heath Consultants Inc., www.heathus.com) is the only current industry standard Hi Flow sampler, it draws air at between 226 and 297 l min^{-1} and can measure CH_4 emissions between 50 g CH_4 h^{-1} to 9 kg CH_4 h^{-1} to an accuracy of ± 10% (Connolly et al., 2019). A recent study commissioned by the California Air Resources Board developed open-source architecture for a new Hi Flow unit which is capable of replacing the current Bacharach Hi Flow Sampler (Vaughn et al., 2022).

$$Q = F.(X_s - X_b) \qquad \text{(Equation 3)}$$

As the Hi-Flow sampler method is relatively simple, no data is required other than the direct measurements made by the instrument. Following the methods of Pekney et al. (2018), the bag containing the hose end of the Bacharach Hi-Flow sampler ~~(Heath Consultants Inc., www.heathus.com)~~ was placed over the point source and the instrument was turned on. This was repeated three times and the average emission calculated. The Hi-Flow sampler used in this study was calibrated monthly as recommended by the manufacturer. This experiment is repeated three times.

2.4 Gaussian Plume

In some circumstances, access and safety restrictions mean that direct measurements are impossible, and an observer must use a far-field method to measure the emissions remotely. The most widely used of these far-field approaches is the Gaussian plume (GP) model. First used in the 1940s, a GP model describes the concentration of a gas as a function of distance downwind from a point source (Seinfeld and Pandis, 2016). When a gas is emitted from the source, it is entrained in the prevailing ambient air flow and disperses laterally and vertically with time, forming a dispersed concentration cone. The concentration enhancement of the gas (X, µg m^{-3}), at any point x meters downwind of the source, y meters laterally from the center line of the plume and z meters above ground level can be calculated (Equation 4) using the emission rate (Q, g s^{-1}), the height of the source (h_s, m) and the Pasquill-Gifford stability class (PGSC) as a measure of air stability. The standard deviation of the lateral (σ_y, m) and vertical (σ_z, m) mixing ratio distributions are calculated from the PGSC of the air (Pasquill, 1962; Busse and Zimmerman, 1973; US EPA, 1995). The GP model assumes that the vertical eddy diffusivity and wind speed are constant and there is total reflection of CH_4 at the surface, where gas reflected from the surface of the Earth is accounted for in the downwind plume. The enhancement is defined as the difference between the downwind concentration and the background concentration measured upwind. The GP is the simplest of the far-field methods considered here and assumes that the emissions are well-defined plumes injected above the near-surface

turbulent layer from point sources and not affected by aerodynamic obstructions that cause mechanical turbulence at the surface. However, in most situations there are aerodynamic obstacles and plumes are rarely perfectly Gaussian in shape. Another shortcoming of the GP model is the parameterization of the PGSC, which are discrete values and incorrectly assigning them can lead to significant uncertainty. Generally, speaking the GP is rarely used for emissions less than 100 g CH4 h^{-1}. However, an example of using a GP model is its use estimating CH_4 emissions from oil production platforms in the North Sea, where emissions ranged from 10 to 80 kg CH_4 hr^{-1} with an uncertainty of ± 45% (Riddick et al., 2019b).

$$\underline{X}(x,y,z) = \frac{Q}{2\pi u \sigma_y \sigma_z} e^{-\frac{y^2}{(2\sigma_y)^2}} \left(e^{-\frac{(z-h_S)^2}{(2\sigma_z)^2}} + e^{-\frac{(z+h_S)^2}{(2\sigma_z)^2}} \right) \qquad \text{(Equation 4)}$$

The GP model uses downwind measurement coupled with meteorology to estimate the emission rate of a source using equation 4. Explicitly, the data used are wind speed (u, m s^{-1}), wind direction (WD, °), temperature (T, °C), CH_4 concentration downwind of the source (X, µg m^{-3}), location and height of the CH_4 detector, background CH_4 concentration (X_b, µg m^{-3}) and the Pasquill-Gifford stability class (PGSC).

Methane emissions are calculated using CH_4 concentrations measured 1.5 m above ground level, 5 m downwind and background CH_4 concentrations 5 m upwind of the source by the Picarro GasScouter. Here, it assumed that the experiments are conducted as close as possible to the source without direct access to the emission point. Wind speed and wind direction were measured every 10 s using a Kestrel 5500 weather meter (www.kestrelmeters.com) on a mast 2 m above the ground. To reduce any impact of mechanical turbulence while maintaining real changes to CH_4 emission caused by changing environmental or atmospheric factors, both CH_4 concentrations and meteorological data are averaged over 15 min (Laubach et al., 2008; Flesch et al., 2009). The PGSC was calculated from the meteorological data using the method of Seinfeld and Pandis (2006). The lookup table, Table S1, is presented in Supplementary Material Section 1. Complex topography, such as building and trees, are not parameterized or accounted for by the GP model.

2.5 bLS dispersion model point measurements

As an alternative to the GP model, Lagrangian dispersion models can be used to calculate the emission of a source. In a backward Lagrangian stochastic (bLS) model, the measurement position, gas concentration, meteorology and micrometeorology are known inputs and the model works iteratively backwards to simulate the motion of the air parcel, this is then used to infer the rate of emission from the source (Flesch et al., 1995). For given meteorological conditions, the model calculates the ratio of downwind concentration to emission, $(C/Q)_{sim}$, depending on the size and location of the source. The emission rate (Q, g m^{-2} s^{-1}) is then inferred from the measured gas concentration at 1.2 m above ground level (X_m, g m^{-3}) and the background gas concentration (X_b, g m^{-3}) (Equation 5). The bLS models can be used to calculate the emissions from point or area sources in a range of micrometeorological conditions. However, a major shortcoming of the model is its inability to adequately model emissions from sources with complex topography or near large objects, such as buildings. This can be mitigated by measuring far away from the source over a relatively flat fetch, but an accurate measurement of the micrometeorology is required. As an example, CH_4 emissions from individual point sources on oil and gas infrastructure have been estimated using a bLS model between 4 µg CH_4 hr^{-1} and 3 kg CH_4 hr^{-1} with an uncertainty of ± 38% (Riddick et al., 2019a)

$$Q = \frac{X_m - X_b}{\left(\frac{C}{Q}\right)_{sim}} \qquad \text{(Equation 5)}$$

WindTrax (www.thunderbeachscientific.com), a commercial software program, uses a bLS dispersion model to calculate the rate of gas emission from a point, area or line source. In this application, the inversion function of the WindTrax inverse dispersion model version 2.0 was used (Flesch et al., 1995). Data used as input are wind speed (u, m s^{-1}), wind direction (WD, °), temperature

(T, °C), downwind CH_4 concentration (X, µg m^{-3}), location and height of the CH_4 detector, background CH_4 concentration (X_b, µg m^{-3}), the roughness length (z_0, m) and the Pasquill-Gifford stability class. The ideal terrain for WindTrax modelling is an obstruction-free surface (Sommer et al., 2005; Laubach et al., 2008)~~(Sommer et al., 2005; Laubach et al., 2008)~~ with the maximum distance between the source and the detector of 1 km (Flesch et al., 2005, 2009)~~(Flesch et al., 2005, 2009)~~. The roughness length was set at 2.3 cm to represent the short grass of the fetch. Again, it assumed that the experiments are conducted as close as possible to the source without direct access to the emission point. Data for downwind average CH_4 concentration, background CH_4 concentration, meteorological and micrometeorological data used in WindTrax will be the same as described in Section 2.4.

2.6 Measures of accuracy and precision

To gain a better understanding of method accuracy and precision, experiments described in sections 2.1 to 2.5 are repeated twice more. In each individual experiment the difference between the known emission rate and the calculated emission rate will be presented as a percentage (Equation 6), where A is the accuracy, Q_c is the calculated emission and Q_k is the known emission. The average accuracy of the three experiments (A_r, %) will be presented as a measure of the accuracy and the standard deviation ($A_{S.D.}$) of the individual uncertainties will be used as a comparative measure of the precision.

$$A = \frac{(Q_c - Q_k)}{Q_k} x\ 100 \qquad \text{(Equation 6)}$$

3 Results and discussion

3.1 Method narrative – anecdotal description of methods

Of the methods tested in this study (summary in Table 1), the static chamber is logistically the simplest. The researcher fixes a container around an emission source and extracts air samples at known time intervals. These vials can be stored for up to a month before analysis on a gas chromatograph. As such, the samples can be analyzed by a third party and the researcher only requires access to the flux chamber, LEL sensor, and the required gas sampling equipment. We found the main shortcomings of the static chamber method are: 1. It was difficult to take samples fast enough during the linear change in concentration; and 2. The method is inherently dangerous.

To address the first shortcoming, a trace gas analyzer could be used to measure the concentrations inside the chamber. As trace gas analyzers use a pump to draw air into the measurement cavity, the analyzer could be arranged in one of two ways. Both introduce additional uncertainty into the quantification. If the gas is removed from the chamber (i.e. the analyzer outlet is vented outside the chamber), the static chamber becomes a dynamic chamber and the analyzer flow rate must be accounted for in the quantification. If the measured gas is reintroduced to the chamber (i.e. the analyzer outlet is vented back to the chamber), a gas of lower concentration is being continually added to the "closed" system and it is therefore unclear how much uncertainty is caused by this cycling. Furthermore, the linear response of a portable trace gas analyzer, e.g. the ABB GLA131-GGA Greenhouse Gas Analyzer (https://new.abb.com/), is 100 ppm. Using the lowest emission rate in the study, 40 g CH_4 h^{-1}, and the largest chamber, 0.5 m^3, the concentration inside the chamber will exceed the linear range within 7 seconds. It is unlikely that gas will mix entirely throughout the chamber in 7 seconds and emission estimates are unlikely to be accurate. Another alternative could be using a lower precision sensor with a larger detection range, such as the SGX INIR- ME100 (https://sgx.cdistore.com/) that can measure from 200 ppm to 100% methane bv, but safety issues remain.

We were aware throughout the experiment that the chamber will become explosive and pre-calculated the time between sample measurement based on the emission rate. During the 200 g CH_4 h^{-1} experiment, the lower explosive limit of CH_4 was reached after three minutes of the chamber being sealed. We would like to highlight that collecting unprocessed natural gas that may contain aromatic hydrocarbons and hydrogen sulphide is ill-advised and we do not recommend its use. As such, we have not presented our measurement data and strongly encourage the use of an alternative method. The static chamber could be automated to release gas when CH_4 concentration inside the chamber approaches LEL to prevent chamber becoming explosive. The major shortcoming of this strategy is that the automation of a chamber takes away the operator's control of when gas is released, which could happen at an inconvenient during measurement. If an automated system is used for collecting gas of unknown composition self-contained breathing apparatus should be worn.

Table 1 Condensed description of logistical needs and results of each experiment. *Access* describes if physical access to the emission source is required (Y denotes having permission to touch/enclose the emission point and N denotes experiments are conducted as close as possible to the source without direct access), *Inst* describes if a dedicated instrument is required, and *C~~c~~ost* is the approximate cost of the lowest price instrument capable of the measurements. *Met* describes if meteorological data is required. T_{meas} and $T_{analysis}$ are the times it takes to conduct and analyse one measurement, respectively. *A* is the accuracy of one measurement of a 200 g CH_4 h^{-1} source (as defined above in Section 2.6), A_r is the average accuracy when repeating the measurement of a 200 g CH_4 h^{-1} source three times, $A_{S.D.}$ is the standard deviation of the accuracy of the three repeated experiments and *U* is the theoretical uncertainty as presented in previous studies.

Method	*Access*	*Inst*	*Cost* (k$)	*Met*	T_{meas} (mins)	$T_{analysis}$ (mins)	*A* (%)	A_r (%)	$A_{S.D.}$	*U (%)*
Static chamber	Y	N	◊-	N	-	-	-	-	-	~~+100, -50~~*
Dynamic chamber	Y	N	◊-	N	15	5	-11	-10	5.9	± 7#
Hi Flow	Y	Y	5	N	5	-	-16	-18	8.2	± 10†
Gaussian Plume	N	Y	32	Y	15	60	33	29	12.5	± 18‡
bLs model	N	Y	32	Y	15	90	-11	-7	14.1	± 12§

~~* Kang et al. (2014),~~ # Riddick et al. (2019), † Pekney et al. (2015), ‡ Riddick et al. (2020), § Riddick et al. (2016)

- the static chamber data is not presented as the method was found to be inherently dangerous.

◊ Cost of sample analysis by GC will vary by laboratory.

The dynamic chamber is logistically one step more advanced than the static chamber and requires a pump to draw air through the chamber at a known rate, and, ideally, a flow meter to measure the air flow. This reduces the potential for CH_4 concentration inside the chamber becoming explosive. This means the main advantages of the static chamber are preserved, i.e. cost and ease of analysis, but mitigates the health and safety concerns. Again, the major shortcoming of the dynamic chamber method is that it requires direct access to the emission source and a 12 V power source for the pump.

The Hi Flow is an off-the-shelf method/instrument, and as an integrated solution, is easier than the dynamic chamber. Once calibrated, the Hi Flow bag is loosely cinched around the emission source and turned on. The instrument displays the methane emission, in l min^{-1}, within a minute at a precision of one significant figure. The data are stored in the instrument and can be downloaded later. The advantages of the Hi Flow are the ease of use and amount of time needed to measure a source, typically five minutes per emission source. The main shortcomings are that the researcher needs to have a Hi Flow instrument, direct access to the source, calibration gas, and a means of charging batteries and/or powering the instrument.

Measurement data required for the GP and bLs methods were the same. After CH_4 is emitted from a source it quickly disperses and to measure the concentration downwind access to a sub-ppm CH_4 analyzer is required. In 2020, the least-expensive, suitable instrument on the market costs around $32,000. In addition to near-ambient CH_4 concentration measurements, meteorological data are required to populate the models. Despite the cost and time required to make the measurements, the practical advantages of these methods are that access is not required, emissions can be calculated from remote sources and that conditions are generally safe. However, ensuring that the measurement location is in the plume for long enough to detect an enhancement large enough for the instrument to measure accurately can be challenging. In light winds the plume can move laterally and the sensor becomes offset.

3.2 Accuracy and precision of repeat measurements

~~Repeating the experiments three times and generating an average value A_r, generally became closer to zero as the flow rate of the source increased.~~ Our results show that the most accurate method for generating emissions after repeat measurements from a 200 g CH_4 h^{-1} source was the bLs method (-7%), then the dynamic chamber (-10%) and then the Hi Flow (-18%) (Table 1). The least accurate method after repeat measurements was the GP model (29%). ~~For most methods, the dynamic chamber, GP and bLs, the accuracy of the emission estimate improved, i.e. $|A_r| < |A|$, while for the HiFlow the accuracy became slightly worse, i.e. $|A_r| > |A|$.~~ Repeating the experiments improved the accuracy of the emission estimate by 4% for the GP model. Data are all presented in Supplementary Material Section 3.

For the 40 g CH_4 h^{-1} source, repeating the experiments generally improved the accuracy of the emission estimate except for the GP model which became 20% less accurate (Figure 2~~B~~A). Like the accuracy, the precision of the methods became better, i.e. the standard deviation (S.D.) of the individual uncertainties became smaller, as the emission rate of the source increased (Figure ~~3~~2B). Methods that made measurements while being attached to the source – chamber and Hi Flow methods – were more precise than those that measured remotely – bLs and GP methods.

~~3.2 Accuracy of single measurements~~

~~To simulate typical measurement methods and gain an understanding of how good a 'snapshot' measurement can be, a single measurement was taken from a source of known emission rates: ~40, 100, 200 g CH_4 h^{-1}. The emissions were generated for each source and the percentage difference between measured and known emissions also calculated (A, %). Emissions calculated using the dynamic chamber and HiFlow methods were -11 % and -16 %, respectively (Figure 2A and Supplementary Material Section 2 Table S2). From these measurements, using single measurement data in a Gaussian Plume model generally results in an overestimate of CH_4 emission, between 33 and 104% higher than the actual emission rate. However, $|A|$ decreases as the emission rate increases; $A = -33\%$ for emissionrates of 200 g CH_4 h^{-1}. For the other three methods, dynamic chamber, HiFlow and bLs, the emission generated are an underestimate, lying within 21% of the known emission rate, and not changing with increased emission.~~

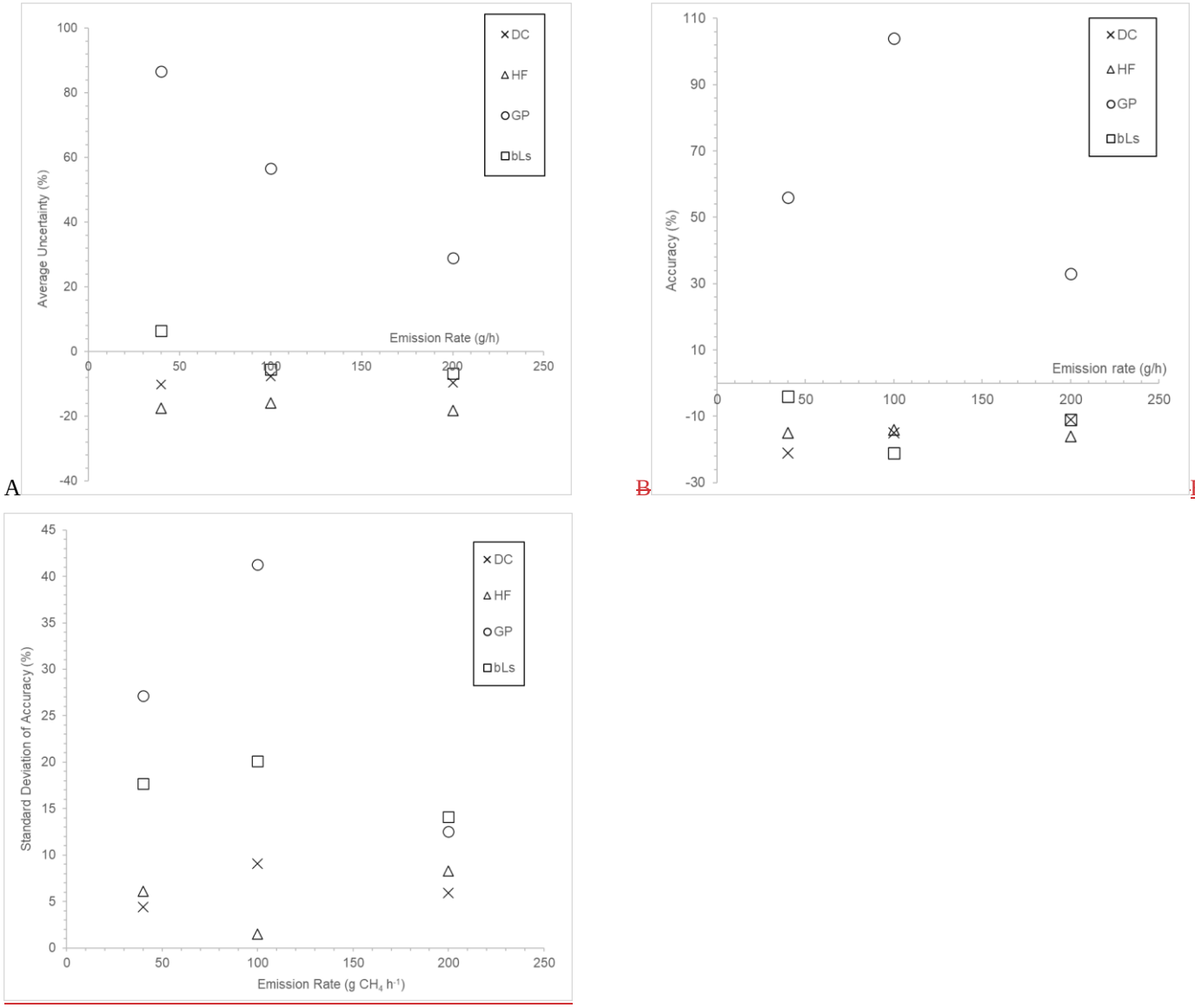

A ~~B~~ ~~B~~

Figure 2~~2~~ A) Average accuracy (% difference from known emission rate) of emission estimates from a ~~single~~ three repeat measurements using each of the measurement methodologies at different known emission rates (~ 40, 100 and 200 g CH_4 h^{-1}). B) The standard deviation of the uncertainties of repeated measurements against the emission rate of the experiment~~Accuracy of emission estimates from the average of three repeated measurements~~. Abbreviations as follows: DC – Dynamic chamber, HF – Hi Flow, GP – Gaussian Plume, bLs – Backwards Lagrangian stochastic method.

~~**3.2 Accuracy and precision of repeat measurements**~~

~~Repeating the experiments three times and generating an average value A_r, generally became closer to zero as the flow rate of the source increased. Our results show that the most accurate method for generating emissions after repeat measurements from a 200 g CH_4 h^{-1} source was the bLs method (~7%), then the dynamic chamber (~10%) and then the HiFlow (~18%) (Table 1). The least accurate method after repeat measurements was the GP model (29%). For most methods, the dynamic chamber, GP and bLs, the accuracy of the emission estimate improved, i.e. $|A_r| < |A|$, while for the HiFlow the accuracy became slightly worse, i.e. $|A_r| > |A|$. Repeating the experiments improved the accuracy of the emission estimate by 4% for the GP model. Data are all presented in Supplementary Material Section 3.~~

~~For the 40 g CH_4 h^{-1} source, repeating the experiments generally improved the accuracy of the emission estimate except for the GP model which became 20% less accurate (Figure 2B). Like the accuracy, the precision of the methods became better, i.e. the S.D.~~

~~of the individual uncertainties became smaller, as the emission rate of the source increased (Figure 3). Methods that made measurements while being attached to the source – chamber and HiFlow methods – were more precise than those that measured remotely – bLs and GP methods.~~

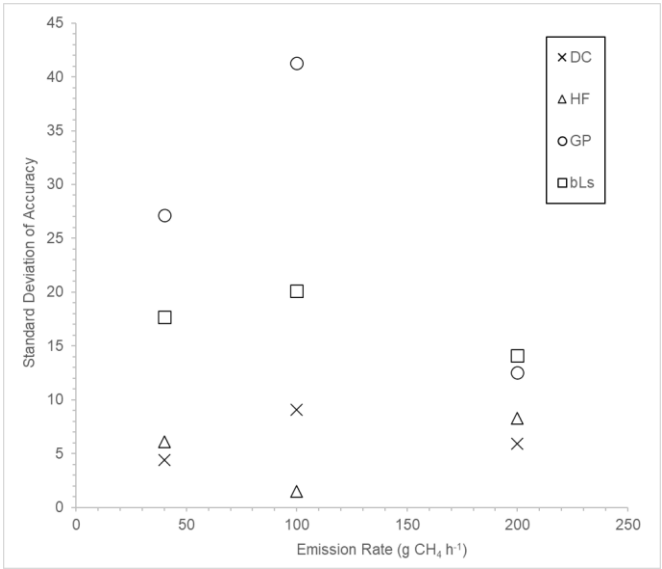

~~**Figure 3 The standard deviation of the uncertainties of repeated measurements against the emission rate of the experiment.**~~

4 ~~Discussion and c~~Conclusions

~~4.1 Precision and accuracy~~

This study investigates the accuracy and precision of five methods that have recently been used to estimate smaller, < 200 g CH_4 h^{-1}, CH_4 emissions from oil and gas infrastructure and include, dynamic chamber, the Bacharach Hi Flow sensor, Gaussian plume modelling and backward Lagrangian stochastic models. Here, we generate CH_4 emission estimates from a known CH_4 source emitting approximately 40, 100 and 200 g CH_4 h^{-1}. Experiments simulating published methods are carried out once to generate a single visit estimate and are then repeated twice more to better understand how repeat experiments can improve the accuracy and precision of the emission estimate.

~~Even though~~Both the dynamic chamber (A_r = -10%, -8%, -10% at emission rates of 40, 100 and 200 g CH_4 h^{-1}, respectively) and Hi Flow (A_r = -18%, -16%, -18%) repeatedly underestimate~~s~~ the emission, ~~i~~but the dynamic chamber is the most accurate for ~~a single~~ measurement~~, which improves with subsequent measurements (A = -11%, A_r = -10%)~~. ~~The HiFlow also underestimates the single emission and becomes less accurate with repetition (A = -16%, A_r = -18%). We suggest the dynamic chamber and HiFlow may be more accurate as the flow of air results in increased mixing within the chamber and the sampled air is a better representation of a homogenous gas mixture.~~

~~F~~For the far field methods, the bLs method underestimated emissions ~~both for single and repeat measurements (A = -11%,~~ (A_r = +6%, -6%, -7%) while the GP method significantly overestimated the emissions (~~A = 33%,~~ A_r = +86%, +57%, +29%) despite using the same meteorological and concentration data as input. These findings are consistent with another study (Bonifacio et al., 2013), however, this is the first study that has compared both to a known emission rate. In all cases the accuracy in the emission estimate increased with emission rate apart from the Hi Flow. The Bacharach Hi Flow system is designed to measure emission from 50 g CH_4 h^{-1} to 9 kg CH_4 h^{-1} to an accuracy of ± 10%. All flow rates presented here are at the lowest range that the Hi Flow can measure and it is likely that the uncertainty in the systems sensors that measures between 40 and 400 g CH_4 h^{-1} is of negligible difference.

The method that improves the most as the emission rate increases is the GP method, where accuracy increases from +87% to +29% as the emission rate increased from 40 to 200 g CH_4 h^{-1}. This improvement in emission is likely caused by the increased size of the plume and the ability of GP model to parameterize the concentration at distances from the centerline of the plume. Although not explicitly stated, the parameterization of the lateral dispersion in the GP model is the same at 100 m as at 5 m which is unlikely. Other controlled release experiments using the GP approach show similar uncertainties, one experiment reported average emissions calculated using a GP model less than 20% (release rates were not published), with the uncertainty mainly driven by atmospheric variability (Caulton et al., 2019). Another showed uncertainties of ±50% for triplicate measurements of emissions between 90 and 970 g CH_4 h^{-1} (Caulton et al., 2018).

Data do not exist on controlled release experiments using a dynamic chamber. One study suggested a theoretical emissions uncertainty in the dynamic chamber approach of ±7% (Riddick et al., 2019a), with the largest source of uncertainty caused by the measurement of the flow rate of air through the chamber. Other sources of uncertainty for the dynamic chamber methods are relatively negligible as the methane quantification of the background gas and the gas at steady state (assuming complete mixing of the gas in the chamber) using the GC is highly accurate over a large concentration range and the volume of the chamber fixed by a plastic structure.

A controlled release has been conducted for the bLs model, but only for an emission from an area source (Ro et al., 2011) at the surface and not analogous to the emissions of this study. Ro et al. (2011) estimated the bLs uncertainty at ± 25% for a gas emitted at an unspecified rate from a 27 m^2 emission area. As with the GP approach, the bLs model's main source uncertainty is the parameterization of the atmospheric stability (Riddick et al., 2012; Flesch et al., 1995; Ro et al., 2011). The main advantage of the bLs model over the GP at these short distances is it calculates the lateral dispersion of gas for individual particles, while the GP uses an averaged dispersion parameter.

The emission estimates quantified using direct methods, dynamic chamber and Hi Flow sampler, have a lower S.D. than the far-field methods (Figure 2B). The S.D. of direct measurement methods remain relatively constant for emissions between 40 and 200 g CH_4 h^{-1} and reflects the relative simplicity of the methods. Assuming all other parameters are measured correctly, for direct methods the variability in emission estimate is a function of how well the CH_4 is mixed into the air in the chamber during the measurement.

Variability in the far field emission estimates is much larger an reflects the relative complexity of inferring emissions. Variability in wind speed, wind direction and atmospheric stability over the 20-minute averaging period are likely to propagate through to large variability in the emission estimate. It may be reasonable to suggest that the variability in bLs calculated emission less than for the GP method because of the added parametrization available (roughness length and gas species). In summary, the penalty of downwind measurement is a higher uncertainty in individual measurements, but this appear to be corrected for by the bLs model through repeat measurements where uncertainty is corrected for by the stochastic nature of particle movement modelling.

~~4.2 Which method to use – a decision making paradigm~~

Regardless of accuracy and precision, this study shows that all methods can be used to estimate emissions from a source ~~less than~~between 40 and 200 g CH_4 h^{-1} to an accuracy of at least 40%. It is reasonable to assume that this level of uncertainty is acceptable in some studies where the research is only aiming to determine relative sizes of emission, e.g. Riddick et al. (2019), while other studies require time-resolved emission estimates to compare against modelled output, e.g. Riddick et al. 2017.

It is, however, concerning that many of the methods show a bias in measurement results and in particular the GP model (Figure 3). In most studies, it is assumed that ~~averaging large numbers of~~in taking multiple measurements ~~reduces~~ the average uncertainty will be reduced to an aggregate, unbiased emission estimate. Taking the GP emission estimates as an example, the individual calculated emissions are all overestimates of the true emission, therefore, suggesting a fundamental shortcoming in the method (Figure 3). These measurements were taking four days apart in similar environmental conditions (all PGSC C) with wind direction being the only difference between measurements, which can be seen from the correlation between the uncertainty and horizontal distance from plume center (Figure 3B). As mentioned above, it is likely that this is due to the lateral dispersion in the GP approach being parametrized incorrectly, i.e. using values that were defined for distances of 100 m ~~error *in the mean* for the measured locations – for example, for a study that surveyed with a downwind method at many well pads, it is generally assumed that, while reported results may be inaccurate for any one facility, the aggregate emission rate across all facilities is an unbiased estimate of total emissions. For the downwind methods and conditions in this study~~This suggests that using the GP approach for distances less than 100 m, ~~this~~ it is not ~~a~~ correct to ~~assumption~~ assume that repeat measurements will remove bias in the calculated average emission~~for most of the methods, and, in particular, will result in substantial error for studies relying on the GP method~~.

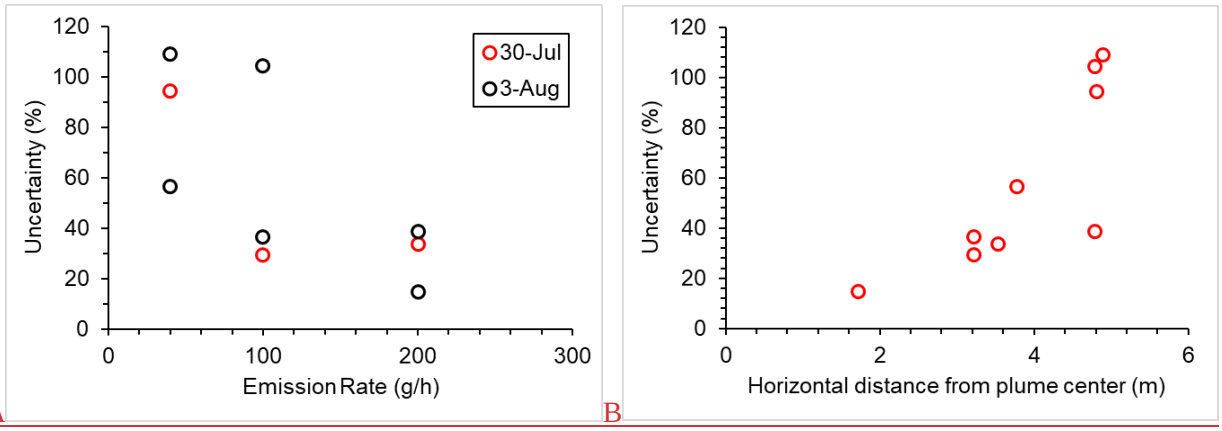

Figure 3 A) Individual uncertainty in Gaussian Plume measurements at 40, 100 and 200 g CH_4 h^{-1} and B) Individual uncertainties plotted against the horizontal distance from the plume center (m)

It is also important to note that the study performed here did not simulate or account for issues which increase error in field conditions. For example, when using downwind methods (GP or bLs), the scientist may not know the exact location of the emission point and may be further downwind of the emission location. These knowledge errors may result in uncertainties, or bias in excess of what is presented here; our study should be viewed as a best case bound on the accuracy of the methods.

~~To provide our findings with some form of context we present our data as a flow diagram to help researchers decide on a suitable method based on accuracy, precision and effort (Figure 4). Here, we give suggestions of which methods could be used given practical and logistical circumstances, i.e. site access and instrument availability. If precision is important in an experiment, our flow diagram would direct a researcher to either the dynamic chamber or the bLs model, while time limitation would suggest the HiFlow. We also hope that the findings of our study could help industry better understand the veracity of researcher's findings and to help put findings in context. As such, we present data that can be used quickly to provide meaning, and balance, to studies that present unexpected findings.~~

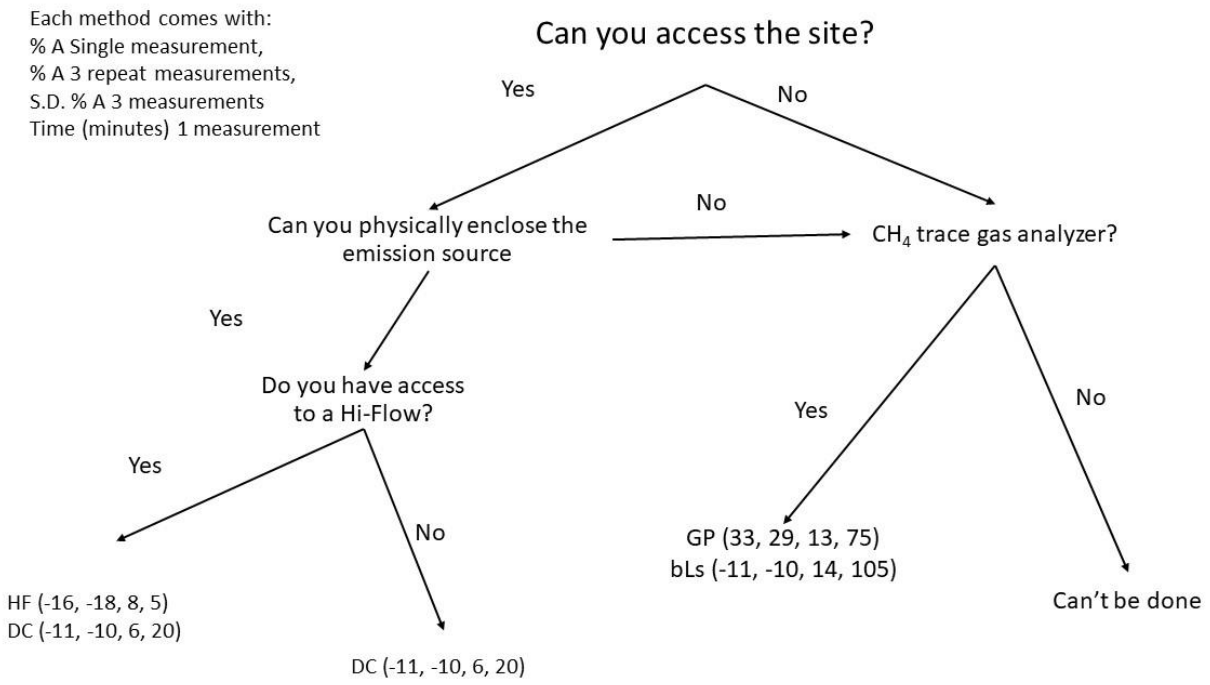

~~**Figure 4 Data presented as a flow diagram to help researchers decide on a suitable method based on accuracy, precision and effort**~~

Author Contributions

Stuart N. Riddick: Conceptualization, Investigation, Methodology, Supervision, Writing – original draft preparation, review and editing

Riley Ancona: Investigation, Data Curation and Analysis, Writing: original draft preparation

Clay Bell: Writing – Analysis, review and editing

Aidan Duggan: Investigation

Tim Vaughn: Investigation, Methodology

Kristine Bennett: Writing – Analysis, review and editing

Dan Zimmerle: Writing – Analysis, review and editing

Stuart N. Riddick: Conceptualization, Investigation, Methodology, Supervision, Writing – original draft preparation, review and editing

Acknowledgements

This work was funded by the METEC Industry Advisory Board (IAB) at Colorado State University.

Competing Interests

The authors declare that they have no conflict of interest.

Disclosure Statement

The authors declare that no financial interest or benefit that has arisen from the direct applications of this research.

References

Allen, D. T., Torres, V. M., Thomas, J., Sullivan, D. W., Harrison, M., Hendler, A., Herndon, S. C., Kolb, C. E., Fraser, M. P., Hill, A. D., Lamb, B. K., Miskimins, J., Sawyer, R. F., and Seinfeld, J. H.: Measurements of methane emissions at natural gas production sites in the United States, Proceedings of the National Academy of Sciences, 110, 17768–17773, https://doi.org/10.1073/pnas.1304880110, 2013.

Aneja, V. P., Blunden, J., Claiborn, C. S., and Rogers, H. H.: Dynamic Chamber System to Measure Gaseous Compounds Emissions and Atmospheric-Biospheric Interactions, in: Environmental Simulation Chambers: Application to Atmospheric Chemical Processes, 97–109, 2006.

Baillie, J., Risk, D., Atherton, E., O'Connell, E., Fougère, C., Bourlon, E., and MacKay, K.: Methane emissions from conventional and unconventional oil and gas production sites in southeastern Saskatchewan, Canada, Environ. Res. Commun., 1, 011003, https://doi.org/10.1088/2515-7620/ab01f2, 2019.

Bell, C. S., Vaughn, T. L., Zimmerle, D., Herndon, S. C., Yacovitch, T. I., Heath, G. A., Pétron, G., Edie, R., Field, R. A., Murphy, S. M., Robertson, A. M., and Soltis, J.: Comparison of methane emission estimates from multiple measurement techniques at natural gas production pads, 5, 79, https://doi.org/10.1525/elementa.266, 2017.

Bonifacio, H. F., Maghirang, R. G., Razote, E. B., Trabue, S. L., and Prueger, J. H.: Comparison of AERMOD and WindTrax dispersion models in determining PM_{10} emission rates from a beef cattle feedlot, Journal of the Air & Waste Management Association, 63, 545–556, https://doi.org/10.1080/10962247.2013.768311, 2013.

Boothroyd, I. M., Almond, S., Qassim, S. M., Worrall, F., and Davies, R. J.: Fugitive emissions of methane from abandoned, decommissioned oil and gas wells, 547, 461–469, https://doi.org/10.1016/j.scitotenv.2015.12.096, 2016.

Brantley, H. L., Thoma, E. D., and Eisele, A. P.: Assessment of volatile organic compound and hazardous air pollutant emissions from oil and natural gas well pads using mobile remote and on-site direct measurements, Journal of the Air & Waste Management Association, 65, 1072–1082, https://doi.org/10.1080/10962247.2015.1056888, 2015.

Caulton, D. R., Shepson, P. B., Santoro, R. L., Sparks, J. P., Howarth, R. W., Ingraffea, A. R., Cambaliza, M. O. L., Sweeney, C., Karion, A., Davis, K. J., Stirm, B. H., Montzka, S. A., and Miller, B. R.: Toward a better understanding and quantification of methane emissions from shale gas development, 111, 6237–6242, https://doi.org/10.1073/pnas.1316546111, 2014.

Caulton, D. R., Li, Q., Bou-Zeid, E., Fitts, J. P., Golston, L. M., Pan, D., Lu, J., Lane, H. M., Buchholz, B., Guo, X., McSpiritt, J., Wendt, L., and Zondlo, M. A.: Quantifying uncertainties from mobile-laboratory-derived emissions of well pads using inverse Gaussian methods, Atmos. Chem. Phys., 18, 15145–15168, https://doi.org/10.5194/acp-18-15145-2018, 2018.

Caulton, D. R., Lu, J. M., Lane, H. M., Buchholz, B., Fitts, J. P., Golston, L. M., Guo, X., Li, Q., McSpiritt, J., Pan, D., Wendt, L., Bou-Zeid, E., and Zondlo, M. A.: Importance of Superemitter Natural Gas Well Pads in the Marcellus Shale, Environ. Sci. Technol., 53, 4747–4754, https://doi.org/10.1021/acs.est.8b06965, 2019.

Collier, S. M., Ruark, M. D., Oates, L. G., Jokela, W. E., and Dell, C. J.: Measurement of Greenhouse Gas Flux from Agricultural Soils Using Static Chambers, JoVE, 52110, https://doi.org/10.3791/52110, 2014.

Connolly, J. I., Robinson, R. A., and Gardiner, T. D.: Assessment of the Bacharach Hi Flow® Sampler characteristics and potential failure modes when measuring methane emissions, Measurement, 145, 226–233, https://doi.org/10.1016/j.measurement.2019.05.055, 2019.

Cooper, J., Dubey, L., and Hawkes, A.: Methane detection and quantification in the upstream oil and gas sector: the role of satellites in emissions detection, reconciling and reporting, Environ. Sci.: Atmos., 2, 9–23, https://doi.org/10.1039/D1EA00046B, 2022.

Denmead, O. T.: Approaches to measuring fluxes of methane and nitrous oxide between landscapes and the atmosphere, Plant Soil, 309, 5–24, https://doi.org/10.1007/s11104-008-9599-z, 2008.

Duren, R. M., Thorpe, A. K., Foster, K. T., Rafiq, T., Hopkins, F. M., Yadav, V., Bue, B. D., Thompson, D. R., Conley, S., Colombi, N. K., Frankenberg, C., McCubbin, I. B., Eastwood, M. L., Falk, M., Herner, J. D., Croes, B. E., Green, R. O., and Miller, C. E.: California's methane super-emitters, Nature, 575, 180–184, https://doi.org/10.1038/s41586-019-1720-3, 2019.

Edie, R., Robertson, A. M., Field, R. A., Soltis, J., Snare, D. A., Zimmerle, D., Bell, C. S., Vaughn, T. L., and Murphy, S. M.: Constraining the accuracy of flux estimates using OTM 33A, Atmos. Meas. Tech., 13, 341–353, https://doi.org/10.5194/amt-13-341-2020, 2020.

Flesch, T., Wilson, J., Harper, L., and Crenna, B.: Estimating gas emissions from a farm with an inverse-dispersion technique, Atmospheric Environment, 39, 4863–4874, https://doi.org/10.1016/j.atmosenv.2005.04.032, 2005.

Flesch, T. K., Wilson, J. D., and Yee, E.: Backward-Time Lagrangian Stochastic Dispersion Models and Their Application to Estimate Gaseous Emissions, J. Appl. Meteor., 34, 1320–1332, https://doi.org/10.1175/1520-0450(1995)034<1320:BTLSDM>2.0.CO;2, 1995.

Flesch, T. K., Harper, L. A., Powell, J. M., and Wilson, J. D.: Inverse-Dispersion Calculation of Ammonia Emissions from Wisconsin Dairy Farms, 52, 253–265, https://doi.org/10.13031/2013.25946, 2009.

Laubach, J., Kelliher, F. M., Knight, T. W., Clark, H., Molano, G., and Cavanagh, A.: Methane emissions from beef cattle - a comparison of paddock- and animal-scale measurements, Aust. J. Exp. Agric., 48, 132, https://doi.org/10.1071/EA07256, 2008.

Livingston, G. P. and Hutchinson, G. L.: Enclosure-based measurement of trace gas exchange: applications and sources of error., in: In: Matson, P.A. and Harris, R.C., Eds., Biogenic trace gases: measuring emissions from soil and water., Blackwell Science Ltd., Oxford, UK, 14–51, 1995.

Nisbet, E. G., Fisher, R. E., Lowry, D., France, J. L., Allen, G., Bakkaloglu, S., Broderick, T. J., Cain, M., Coleman, M., Fernandez, J., Forster, G., Griffiths, P. T., Iverach, C. P., Kelly, B. F. J., Manning, M. R., Nisbet-Jones, P. B. R., Pyle, J. A., Townsend-Small, A., al-Shalaan, A., Warwick, N., and Zazzeri, G.: Methane Mitigation: Methods to Reduce Emissions, on the Path to the Paris Agreement, Rev. Geophys., 58, https://doi.org/10.1029/2019RG000675, 2020.

Pekney, N. J., Diehl, J. R., Ruehl, D., Sams, J., Veloski, G., Patel, A., Schmidt, C., and Card, T.: Measurement of methane emissions from abandoned oil and gas wells in Hillman State Park, Pennsylvania, Carbon Management, 9, 165–175, https://doi.org/10.1080/17583004.2018.1443642, 2018.

Pihlatie, M. K., Christiansen, J. R., Aaltonen, H., Korhonen, J. F. J., Nordbo, A., Rasilo, T., Benanti, G., Giebels, M., Helmy, M., Sheehy, J., Jones, S., Juszczak, R., Klefoth, R., Lobo-do-Vale, R., Rosa, A. P., Schreiber, P., Serça, D., Vicca, S., Wolf, B., and Pumpanen, J.: Comparison of static chambers to measure CH4 emissions from soils, Agricultural and Forest Meteorology, 171–172, 124–136, https://doi.org/10.1016/j.agrformet.2012.11.008, 2013.

Riddick, S. N., Dragosits, U., Blackall, T. D., Daunt, F., Wanless, S., and Sutton, M. A.: The global distribution of ammonia emissions from seabird colonies, 55, 319–327, https://doi.org/10.1016/j.atmosenv.2012.02.052, 2012.

Riddick, S. N., Connors, S., Robinson, A. D., Manning, A. J., Jones, P. S. D., Lowry, D., Nisbet, E., Skelton, R. L., Allen, G., Pitt, J., and Harris, N. R. P.: Estimating the size of a methane emission point source at different scales: from local to landscape, 17, 7839–7851, https://doi.org/10.5194/acp-17-7839-2017, 2017.

Riddick, S. N., Mauzerall, D. L., Celia, M. A., Kang, M., Bressler, K., Chu, C., and Gum, C. D.: Measuring methane emissions from abandoned and active oil and gas wells in West Virginia, 651, 1849–1856, https://doi.org/10.1016/j.scitotenv.2018.10.082, 2019a.

Riddick, S. N., Mauzerall, D. L., Celia, M., Harris, N. R. P., Allen, G., Pitt, J., Staunton-Sykes, J., Forster, G. L., Kang, M., Lowry, D., Nisbet, E. G., and Manning, A. J.: Methane emissions from oil and gas platforms in the North Sea, 19, 9787–9796, https://doi.org/10.5194/acp-19-9787-2019, 2019b.

Riddick, S. N., Mauzerall, D. L., Celia, M., Allen, G., Pitt, J., Kang, M., and Riddick, J. C.: The calibration and deployment of a low-cost methane sensor, Atmospheric Environment, 230, 117440, https://doi.org/10.1016/j.atmosenv.2020.117440, 2020a.

Riddick, S. N., Mauzerall, D. L., Celia, M. A., Kang, M., and Bandilla, K.: Variability observed over time in methane emissions from abandoned oil and gas wells, International Journal of Greenhouse Gas Control, 100, 103116, https://doi.org/10.1016/j.ijggc.2020.103116, 2020b.

Ro, K. S., Johnson, M. H., Hunt, P. G., and Flesch, T. K.: Measuring Trace Gas Emission from Multi-Distributed Sources Using Vertical Radial Plume Mapping (VRPM) and Backward Lagrangian Stochastic (bLS) Techniques, Atmosphere, 2, 553–566, https://doi.org/10.3390/atmos2030553, 2011.

Seinfeld, J. H. and Pandis, S. N.: Atmospheric chemistry and physics: from air pollution to climate change, Third edition., John Wiley & Sons, Inc, Hoboken, New Jersey, 1120 pp., 2016.

Sommer, S. G., McGinn, S. M., and Flesch, T. K.: Simple use of the backwards Lagrangian stochastic dispersion technique for measuring ammonia emission from small field-plots, European Journal of Agronomy, 23, 1–7, https://doi.org/10.1016/j.eja.2004.09.001, 2005.

Townsend-Small, A., Ferrara, T. W., Lyon, D. R., Fries, A. E., and Lamb, B. K.: Emissions of coalbed and natural gas methane from abandoned oil and gas wells in the United States: METHANE EMISSIONS FROM ABANDONED WELLS, 43, 2283–2290, https://doi.org/10.1002/2015GL067623, 2016.

US EPA: Inventory of U.S. Greenhouse Gas Emissions and Sinks 1990-2020: Updates Under Consideration for Abandoned Oil and Gas Wells, 2021.

Vaughn, T. L., Ross, C., Zimmerle, D. J., Bennett, K. E., Harrison, M., Wilson, A., and Johnson, C.: Open-Source High Flow Sampler for Natural Gas Leak Quantification, Contract: 19ISD010, 2022.

Zimmerle, D., Vaughn, T., Bell, C., Bennett, K., Deshmukh, P., and Thoma, E.: Detection Limits of Optical Gas Imaging for Natural Gas Leak Detection in Realistic Controlled Conditions, Environ. Sci. Technol., 54, 11506–11514, https://doi.org/10.1021/acs.est.0c01285, 2020.